BSGF - Earth Sciences Bulletin 2018, 189, 5
© R. Vaucher *et al.*, Published by EDP Sciences 2018
https://doi.org/10.1051/bsgf/2018004

BSGF
Earth Sciences Bulletin
Available online at:
www.bsgf.fr

Bedforms in a tidally modulated ridge and runnel shoreface (Berck-Plage; North France): implications for the geological record

Romain Vaucher[1,2,*], Bernard Pittet[1], Sophie Passot[1], Philippe Grandjean[1], Thomas Humbert[3] and Pascal Allemand[1]

[1] Univ Lyon, Université Claude Bernard Lyon 1, ENS de Lyon, CNRS, UMR 5276 LGL-TPE, 69622 Villeurbanne, France
[2] CICTERRA CONICET, Universidad Nacional de Córdoba, Av. Velez Sarsfield 1611, X5016GCA Córdoba, Argentina
[3] Laboratoire d'Acoustique de l'Université du Maine, UMR6613 CNRS/Univ. du Maine, 72085 Le Mans cedex 9, France

Abstract – Tidally modulated shoreface (TMS) corresponds to peculiar costal environments. The general morphology and the expressed bedforms are provided by the interplay of both waves and tides. The recognition of TMS in the fossil record still remains a difficult task. The study of one mega-tidal modern TMS in the north of France (Berck-Plage) provides new key criteria to identify this kind of coastal system in the rock record. Field investigation and digital mapping were realized at lowest tide during spring tide under fair-weather condition. The intertidal zone is characterized by a succession of several sand banks shore parallel separated by topographic lows that are defined as ridges and runnels. Seven distinct dominant bedforms are recognized: 3D current ripples, 3D asymmetrical ripples, 2D symmetrical ripples, 2D small symmetrical dunes, 2D large symmetrical dunes, 3D symmetrical dunes and plane beds. The upper stage plane bedding mainly composed the ridges while the six other bedforms are commonly found within the runnels or on the flanks of the ridges. Comparison of the bedforms of Berck-Plage with previous experimental studies on bedforms genesis proves that the necessary flow parameters for generating these bedforms belong to an oscillatory flow except for the 3D current ripples, which are formed by a unidirectional flow. This study confirms the dominance of oscillatory structures through the intertidal zone in a mega-tidal context and show that wave processes are more powerful than tide processes for bedform generation although during fair weather conditions. Based on the timing of genesis, the description and the repeated pattern of distribution of bedforms between two ridges is highlighted thus helping to propose a theoretical facies sequence for an intertidal zone characterized by ridges and runnels applicable to ancient sedimentary successions.

Keywords: waves / tides / ridge and runnel / bedforms / stratigraphy / Berck-Plage / France

Résumé – Structures sédimentaires d'une zone intertidale en barre et bâches dominée par la houle (Berck-Plage ; Nord de la France) : implications pour le registre sédimentaire ancien. Les plages et avant-plages sous l'influence de la houle et modulées par l'action de la marée, correspondent à des environnements côtiers particuliers. Leurs géomorphologies générales ainsi que les structures sédimentaires associées résultent de l'action combinée de la houle et de la marée. L'identification de ces environnements atypiques dans des successions sédimentaires anciennes demeure difficile. L'analyse d'un environnement mégatidal semi-diurne actuel dans le Nord de la France (Berck-Plage) a permis de fournir de nouveaux critères de reconnaissance pour ce type de système côtier hybride dans le fossile. Une étude de terrain ainsi qu'une cartographie numérique ont été réalisées à marée basse au cours d'une marée de vives-eaux. La zone intertidale est caractérisée par une succession de plusieurs bancs de sables parallèles à la côte et qui sont définies comme des barres (topographie positive) et des bâches (topographie négative). L'étude de terrain de cette zone a révélé sept types de structures sédimentaires : des rides de courant 3D ; des rides asymétriques 3D ; des rides symétriques 2D ; des petites dunes symétriques 2D ; des grandes dunes symétriques 2D ; des grandes dunes symétriques 3D et des litages plans. Les structures planes caractérisent principalement le

*Corresponding author: romain.vaucher88@gmail.com

sommet des barres, tandis que les six autres types de structures sédimentaires se retrouvent plus communément dans les bâches ou sur le flanc des barres. La comparaison effectuée de la morphologie des structures sédimentaires de Berck-Plage avec celles d'études expérimentales sur la genèse de structures sédimentaires prouve que les paramètres de flux nécessaires sont relatifs à un courant oscillatoire (à l'exception des rides d'asymétriques 3D, qui sont formées par un courant unidirectionnel). Cette étude confirme la prédominance des structures oscillatoires dans la zone intertidale mégatidale et montre clairement que les processus de houle sont plus énergiques que ceux liés aux marées, même en contexte de beau temps. La cartographie de ces sept types de structures sédimentaires montre une répartition similaire des structures entre chaque couple de barres/bâches. Ces observations ont permis de proposer une séquence de faciès théorique pour un environnement mégatidal dominé par la houle qui est utilisable pour la reconnaissance d'environnements similaires dans les successions sédimentaires anciennes.

Mots clés : houle / marée / barre et bâche / structures sédimentaires / stratigraphie / Berck-Plage / France

1 Introduction

Waves and tides are the two main processes acting either separately or together on the formation of sedimentary structures, their repartitions and the geomorphology of coastal systems. Facies models for wave-dominated (*e.g.* Clifton *et al.*, 1971; Harms, 1979; Davis Jr and Hayes, 1984; Davis Jr, 1985; McLane, 1995; Allen, 1997; Plint, 2010) and tide-dominated (*e.g.* Dalrymple, 1992, Dalrymple *et al.*, 2003; Davis and Dalrymple, 2012) sedimentary systems are now well constrained in the literature. Nowadays modern hybrid (wave and tide) sedimentary systems are widespread but they are weakly described or recognized in ancient sedimentary successions (Dalrymple, 2010). Even if recent studies have shown how the co-influence of waves and tides can be recognized in the rock record at different scales, from the sedimentary structures to the general stratigraphic succession in sedimentary sequences (*e.g.* Basilici *et al.*, 2011, 2012; Vakarelov *et al.*, 2012; Rossi and Steel, 2016; Smosna and Bruner 2016; Vaucher *et al.*, 2017) there is a lack of study on modern environment providing key criteria for the recognition of ancient hybrid sedimentary successions. Modern environments have been investigated (*e.g.* Yang and Chun, 2001; Yang *et al.*, 2005, 2006, 2008a, b; Dashtgard *et al.*, 2009, 2012) and the double influence (waves and tides) was clearly pointed out by sedimentological and/or ichnological evidences. These studies on modern environments are mainly based on boxcore analysis, thus giving a vertical (temporal) view to the observations but do not allow to understand the timing of formation of each bedform as well as their lateral evolution. In order to constrain the spatial distribution of sedimentary bodies and their associated bedforms in a tidally modulated modern shoreface (TMS; *sensu* Dashtgard *et al.*, 2009), the Berck-Plage mega-tidal beach in northern France was investigated. It allows providing the spatial repartition of the different bedforms in order to reconstruct an idealized temporal succession of sedimentary structures expected in TMS. The studied area is characterized by several shore-parallel, sand banks that are *ca.* 1 m high (from trough to crest) and spaced from each other by *ca.* 200 m. This beach morphology, called ridge and runnel, was first described by King and Williams (1949). These peculiar beaches were subject to numerous publications that mainly describe their coastal dynamics (*e.g.* Short, 1991; Levoy *et al.*, 1998; Ruessink, 1998; Voulgaris *et al.*, 1998; Sipka and Anthony, 1999; Kroon and Masselink, 2002; Wijnberg and Kroon, 2002; Stépanian and Levoy, 2003; Anthony *et al.*, 2004; Masselink, 2004; Masselink *et al.*, 2006; van Houwelingen *et al.*, 2006; Lashteh Neshaei *et al.*, 2009). However, the associated bedforms generated over the ridges and runnels have less been investigated. Only Chauhan (2000) has studied the different bedforms occurring in such environments.

In this study we propose:

- to describe the bedforms generated in a ridge and runnel mega-tidal context using field investigations and ortho-images analysis, to constrain their spatial distribution and to interpret the hydrodynamic processes generating the bedforms;
- to propose a theoretical vertical stacking pattern of the encountered sedimentary structures, applicable to the rock record, for the intertidal zone of TMS characterized by a ridge and runnel morphology;
- to compare this idealized sequence of facies to an ancient sedimentary succession.

2 Study area

The beach of Berck-Plage (Fig. 1A) is part of the Côte d'Opale in the northern part of France (Pas-de-Calais department) on the English Channel and is elongated on a N-S axis. This beach is submitted to moderate waves (fair-weather waves are < 1.5 m high; storm waves are *ca.* 2–4 m high; Augris *et al.*, 2004) and to a mega-tidal regime (spring tidal range of 8.3 m; Anthony *et al.*, 2004). Macro- and mega-tidal beaches are widespread on all continents, mainly in protected environments even if some are located in exposed environments (oceans) (Short, 1991). Macro- or mega-tidal beaches can be classified in three distinctive groups: (1)higher wave, planar, uniform slope; (2) moderate waves, multi bar; (3) low wave beach and tidal flat (Short, 1991).

Multi bar (*i.e.* ridge and runnel) beaches were first described by King and Williams (1949). This kind of beach is constituted of fine to medium sands, shows a 0.5–0.6° intertidal gradient, and presents several bars disconnected from each other (Short, 1991). The bars usually occur between the mean highest (MHTL) and the mean lowest tide levels (MLTL), have a height < 1 m and are spaced from 50 to 150 m. Several surveys of multi barred costal environments tend to suggest that positions and dimensions of the bars are relatively stable through times (*e.g.* King, 1972; Hale and McCann, 1982).

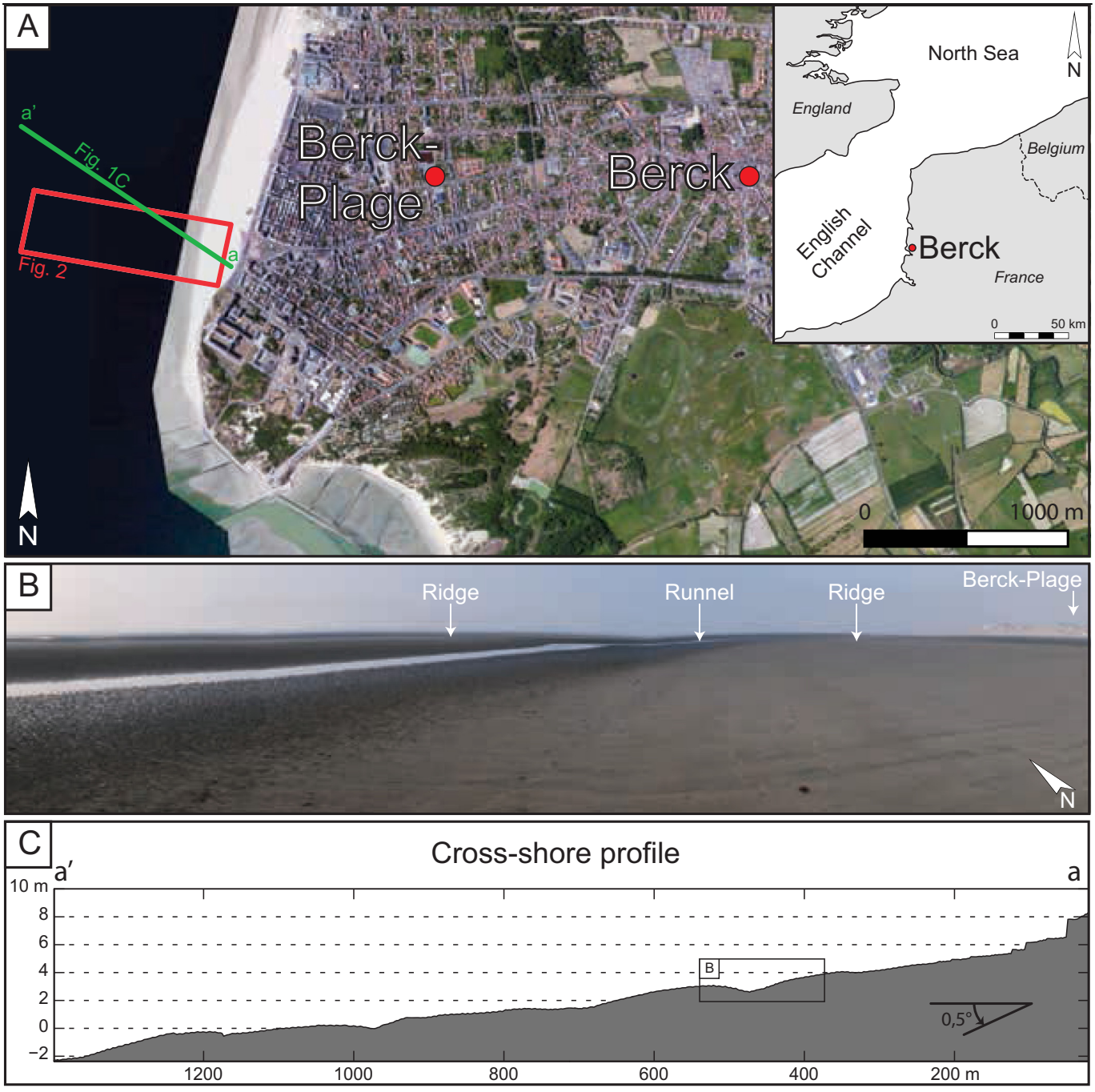

Fig. 1. (A) Satellite image of the study area, from Bing Maps. The study area is a part of the intertidal zone of Berck-Plage (North France) orientated in N-S axis on the English Channel side; red rectangle: location of the ortho-images (see Fig. 2) achieved on the area, covering an area of *ca.* 0.58 km^2. (B) Part of the intertidal zone of Berck-Plage at low tide displaying a ridge and runnel morphology. (C) Cross-shore profile of the intertidal zone showing the ridge and runnel morphology.

Intuitively, the ridges was supposed to be formed by swash action during a stationary water levels (King, 1972), however, a more recent study (*e.g.* Masselink and Anthony, 2001) suggests that both swash and surf processes acting together could be responsible for the development and stability of the ridge and runnel geomorphology. The exact processes responsible of the bar formation remain unknown and other processes such as infragravity waves are invoked for their formation in the intertidal zone (*e.g.* Ruessink, 1998). Associated with these large bars, several bedforms (ripples and dunes) generated by oscillatory-, unidirectional- or combined-flows are also present and can be interpreted in terms of hydrodynamic conditions and relative water depth according to the elevation of the tide and wave action.

The intertidal zone of Berck-Plage consisting of well-sorted fine to medium grained quartz and a small quantity of

bioclasts, has a general slope angle of *ca*. 0.5°, and displays numerous linear shore parallel banks. The Berck-Plage intertidal zone can thus be considered as a ridge and runnel beach (Fig. 1B and C). Five ridges are observed, which display a general asymmetry with a steeper landward than seaward slope. The troughs (runnels) between ridges act as channels during rising and falling tide.

3 Methods

The intertidal zone of Berck-Plage was investigated and analysed under fair-weather conditions during spring tide that reached up to 10 m of tidal range. The different bedforms were described in the field during the lowest tide levels. The spatial distribution and mapping of the observed bedforms were realized on ortho-images (Fig. 2), which covered an area of *ca.* 0.58 km^2 ranging from the MHTL to the MLTL.

3.1 Images acquisition

Images used for the spatial distribution and structure mapping were acquired by drone. The surveys were performed using DRELIO, a drone based on a multi-rotor platform. It is equipped for nadir photography with a reflex camera Nikon D700 with a focal length of 35 mm, taking every 2 seconds one 12 Mpix photo stored in JPEG fine format. The flight in cruise limb is realized in automatic mode at an elevation of 100 m above the intertidal zone. During the cruise limb, DRELIO follows a programmed path that has been prepared and downloaded in its memory just before takeoff. Before each flight, 15 highly visible targets were distributed in the study area. These targets are circular red disks of 23 cm in diameter. They are georeferenced with post-processed Differential GPS (DGPS), using a Topcon HiPer II GNSS receiver. During each flight, more than 250 images were taken. The resolution of the images was around 2 cm.

Images were processed using the MicMac chain in order to obtain DEM and ortho-images of each flight. MicMac (acronym for "Multi-Images Correspondances, Méthodes Automatiques de Corrélation") is an open-source photogrammetric software suite developed by IGN® for computing 3D models from sets of images (Pierrot Deseilligny and Clery, 2011; Pierrot Deseilligny, 2015). The process is realized in four steps. During the first one, tie points are computed on the images using the SIFT++ algorithm. The result of this step is a list of the position of the tie points on each image. In the second step, the external orientation and the intrinsic calibration of the camera are computed assuming a Fraser's radial model of distortion. The results of this step are a set of parameters of distortion and a relative position and orientation of the camera for each image. The third step consists in a dense matching between the images that overlap in order to produce the DEM of the whole surface at a resolution close of the resolution of the image, *i.e.* 2 cm in this case. In the last step, the ortho-image is computed at the same resolution than the DEM. Finally the ortho-images and the DEM are georeferenced in a Lambert93 projection using the position and elevation of the targets visible on the ortho-image. The planimetric precision of the georeferencing is better than 5 cm.

3.2 Bedform nomenclature

Several experimental studies were performed on the genesis of bedforms under unidirectional-, oscillatory- and combined-flows (*e.g.* Dumas *et al.*, 2005; Cummings *et al.*, 2009; Perillo *et al.*, 2014a, b, c). In this study, the bedforms described in the intertidal zone follow the more up-to-date bedform classification provided from Perillo *et al.* (2014a) and was adapted when the bedforms were not present in their study: 3D Current Ripples (3D CR), 3D Asymmetrical Ripples (3D AR), 2/2.5D Symmetrical Ripples (2/2.5SD), 2D Symmetrical Small Dune (2D SSD), Upper-Stage Plan Bed (USPB), 2D Symmetrical Dunes (2D SD), 3D Symmetrical Dunes (3D SD). Only the 2D SSD nomenclature was created since it did not exist in Perillo *et al.* (2014a). The description of the bedforms (Tab. 1) takes into account the crest-to-crest spacing (or wavelength), the elevation (from trough to crest), the bedform symmetry/asymmetry and their general geometry (2D, 2.5D, 3D). Due to the homogeneous nature of the sediments that composed the intertidal zone, no internal sedimentary structures were visible. Once the bedforms described, a map of their distribution (Fig. 2) was achieved under SIG software (Quantion SIG) in order to constrain their relationship to each other.

4 Bedform descriptions and interpretations

Field analysis and ortho-images (Fig. 2) have permitted to define seven bedforms (Figs. 2 and 3) across the intertidal zone of Berck Plage. Their main characteristics of each bedform are summarized in Table 1. The mean flow velocities responsible of the bedforms formation are given by Dumas *et al.* (2005) and Perillo *et al.* (2014a). Two bedforms are found on the ridges only, two in the runnels, and four are generally encountered at the transition runnel-ridge.

4.1 3D CR

Asymmetrical ripples are few centimeters high and display a mean crest-to-crest length of *ca.* 10 cm (Tab. 1; Figs. 3A, D and G). The crest morphology is sinuous and sharp. These bedforms, only present in the lowest part of the runnel, are the less frequently observed in Berck-Plage. Generally, these bedforms are still submerged even during the lowest tidal state. The asymmetrical characteristics of these bedforms suggest they are formed by a unidirectional flow with an associated unidirectional flow velocity (U_c)>10 $cm.s^{-1}$ (*e.g.* Harms, 1979; Dumas *et al.*, 2005; Perillo *et al.*, 2014a). They are described as 3D Current Ripples (3D CR; *sensu* Perillo *et al.*, 2014a). The progradation of the 3D CR is mostly toward the north or the south (following the axes of the runnels); even some are toward the west according to the orientation of the ebb-flow (Fig. 2). The current ripples can feed the troughs of larger bedforms to form small delta-*like* sediment accumulations (dotted white lines; Fig. 3G).

4.2 3D AR

Quasi-asymmetrical/asymmetrical ripples of *ca.* 5 cm high and showing wavelengths of *ca.* 15–20 cm are observed

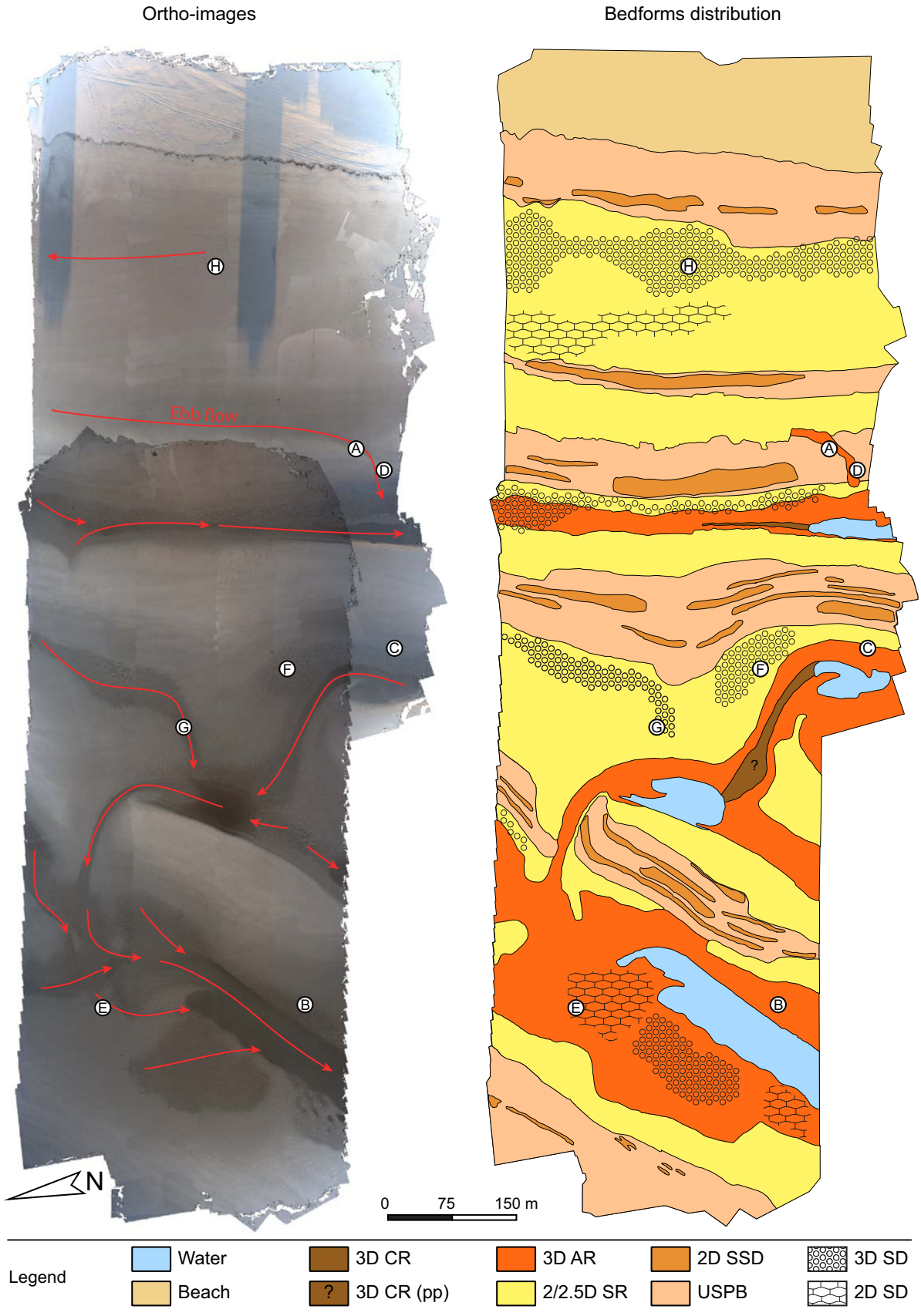

Fig. 2. Ortho-images (left) and bedform distribution (right) in the studied intertidal zone. 3D CR (3D Current Ripples); 3D CR-pp (3D Current Ripples poorly preserved); 3D AR (3D Asymmetrical Ripples); 2/2.5D SR (2/2.5D Symmetrical ripples); 2D SSD (2D Symmetrical Small Dunes); USPB (Upper Stage Plane Bed); 3D SD (3D Symmetrical Dunes); 2D SD (2D Symmetrical Dunes). A to H refer to Figure 3.

Table 1. Summary of the observed bedforms and comparison with two experimental studies (Dumas *et al.*, 2005 and Perillo *et al.*, 2014a). 3D CR (3D Current Ripples); 3D AR (3D Asymmetrical Ripples); 2/2.5D SR (2/2.5D Symmetrical ripples); 2D SSD (2D Symmetrical Small Dunes); USPB (Upper Stage Plane Bed); 3D SD (3D Symmetrical Dunes); 2D SD (2D Symmetrical Dunes). λ(cm) bedform wavelength; η(cm) bedform elevation; U_o (cm.s^{-1}) velocity of oscillatory flow; U_c (cm.s^{-1}) velocity of unidirectional flow; Ø: no data; Abs.: Not observed

	This study				Dumas *et al.*, (2005)				Perillo *et al.*, (2014a)			
Bedforms	λ(cm)	η(cm)	Position along the intertidal zone	% of bedforms trough the intertidale zone	Uo (cm.s^{-1})	Uc (cm.s^{-1})	λ (cm)	η (cm)	Uo (cm.s^{-1})	Uc (cm.s^{-1})	λ (cm)	η (cm)
3D CR	15	2	Trough of runnel	0,6	Ø	> 10	Ø	Ø	< 15	> 20	35	1,5
3D AR	15	5	Trough of runnel / bottom of ridge	12,4	< 40	> 10	11–21	1,2–2,9	15–50	Ø	22	2,5
2/2.5D SR	16	5	Slope / bottom of ridge	31,4	< 40	> 5	7–11	0,5–1,3	< 30	< 10	23	3,7
2D SSD	50	15	Top of the ridge	4,6	Abs. 90–120	Abs. Ø	Abs.	Abs.	Abs.	Abs.	Abs.	Abs.
USPB	Ø	Ø	Top of the ridge	29,7	60	20	Ø	Ø	Ø	Ø	Ø	Ø
2D SD	120	20	Slope / bottom of ridge	3,7	40–100	< 4	111–224	6–27	Abs.	Abs.	Abs.	Abs.
3D SD	140	20–50	Slope / bottom of the ridge	13,7	50–90	< 15	150–300	10–25	70–80	< 20	70	6

(Tab. 1; Fig. 3B and E). The crests are discontinuous, not straight and orientated along NW-SE and SW-NE axes. These bedforms are usually found laterally to the 3D CR on the bottom of the ridges still in the runnel part of the intertidal zone. These bedforms differ from the 3D CR mainly on the rounded aspect of the crest and thus point to a combined-flow (oscillatory dominating) origin with velocity of the oscillatory flow (U_o) between 15–50 cm.s^{-1} and a U_c>10 cm.s^{-1} (*e.g.* Harms, 1979; Dumas *et al.*, 2005; Perillo *et al.*, 2014a). They are described as 3D Asymmetrical Ripples (3D AR; *sensu* Perillo *et al.*, 2014a).

4.3 2/2.5D SR

Symmetrical ripples of a few centimetres high, exhibiting a wavelength of 15 to 20 cm, are also frequently observed (Tab. 1; Fig. 3B, C and G). The crests of the bedforms are orientated along a N-S axis for those found on the top of the slope of the ridges and thus parallel to the shoreline. However, other 2D SR crests showed an E-W axis for the ones in the middle of the slope of the ridges to the beginning of the runnels and are therefore orthogonal respectively to the shoreline (see further in the text for an explanation). The crests are continuous and straight (2D) and/or continuous but not straight (2.5D). These bedforms are usually present at the transition between the ridge and the runnel, higher on the slope of the ridges than the 3D AR. An oscillatory flow is responsible for the formation of these bedforms with a mean U_o > 40 cm.s^{-1} even if current component may occur U_c < 10 cm.s^{-1} (*e.g.* Harms, 1979; Dumas *et al.*, 2005; Perillo *et al.*, 2014a). They are described as 2/2.5D Symmetrical Ripples (2/2.5D SR; *sensu* Perillo *et al.*, 2014a).

4.4 2D SSD

Larger symmetrical ripples compared to 2/2.5D SR of *ca.* 10 cm high, and showing a wavelength of *ca.* 50 cm can be observed at the transition ridge-runnel (Tab. 1, Fig. 2D). The crests are linear and straight, and elongated in a N-S direction, parallel to the shoreline *sensu lato*. According to their symmetrical morphology, an oscillatory flow could be suggested for their formation (*e.g.* Harms, 1979; Dumas *et al.*, 2005; Perillo *et al.*, 2014a). Since this bedform is encountered on the upper slope part of the ridge, between the 2D SR and the USPB (see further in the text), this position corresponds at a giving time, according to the elevation of the tide, to the surf-swash transition zone where supercritical flow likely occurs (Brocchini and Baldock, 2008). Thus, supercritical flow could be responsible of the formation of the 2D SSD similar to those described by Broome and Komar (1979). However, concerning their names, regarding to their dimensions they can be classified either as dunes or ripples by Perillo *et al.* (2014a) (Tab. 1). Here, these bedforms are described as 2D Symmetrical Small Dune (2D SSD) in order to be consistent with the used nomenclature. Intermediate bedforms such as 2D SSD, even if they can be physically generated, were not observed in the experimental study of Dumas *et al.* (2005). However, bedforms equivalent to 2D SSD were present, but not classified, in the experimental study of Perillo *et al.* (2014a).

4.5 USPB

Flat beds are the main observed bedforms on the ridges (Tab. 1, Figs. 1B and 3D). According to the context (an intertidal zone) submitted to constant swash and surf processes, these bedforms are interpreted to be Upper Stage Plane Bed (USPB; *sensu* Perillo *et al.*, 2014a) resulting from a high velocity current with a mean U_c>60 cm.s^{-1} (swash and backwash).

4.6 2D SD

Large symmetrical bedforms of *ca.* 20 cm high and displaying a wavelength of *ca.* 120 cm, are present in the

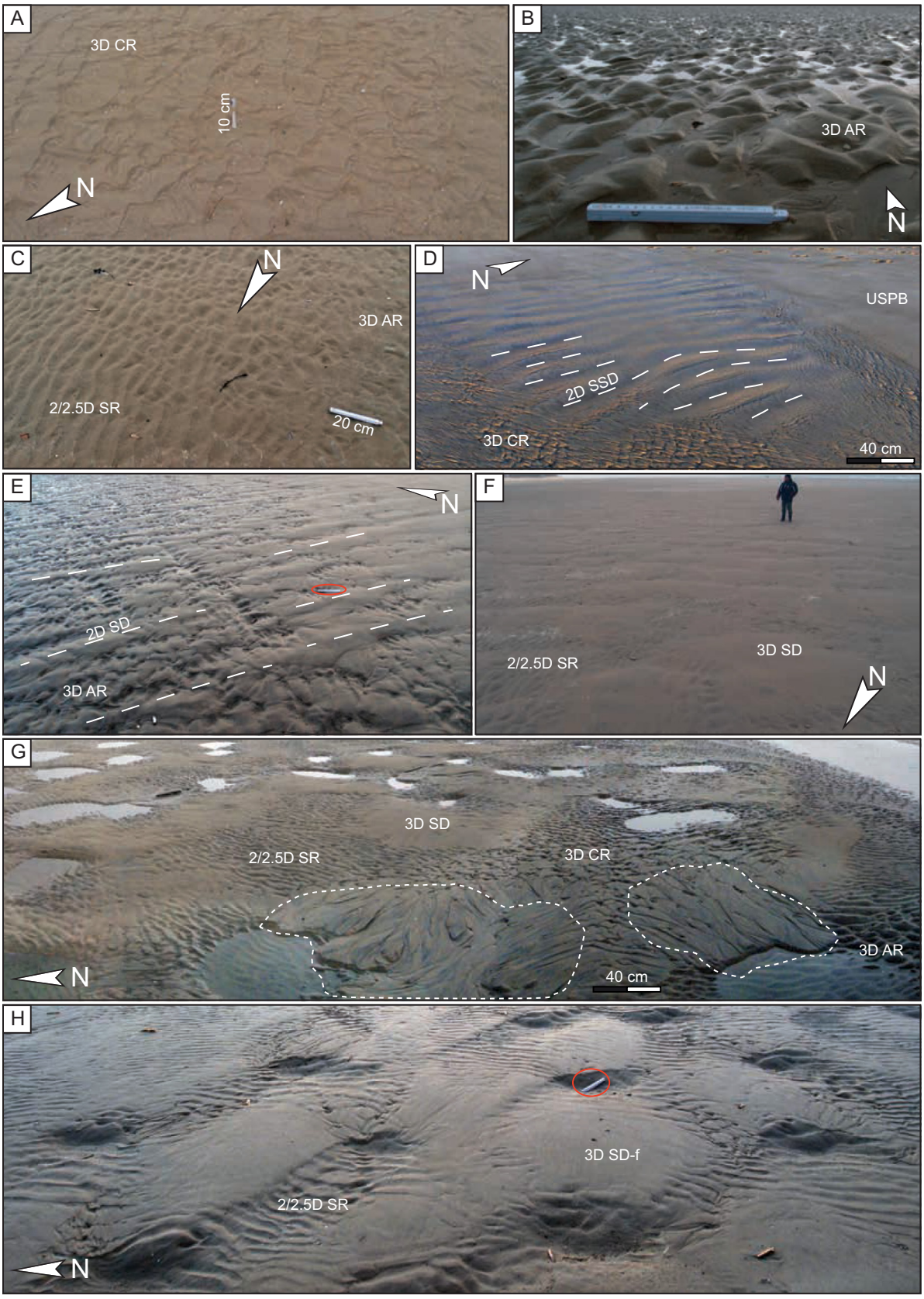
A
3D CR
10 cm
N
B
3D AR
N
C
N
3D AR
2/2.5D SR
20 cm
D
N
USPB
2D SSD
3D CR
40 cm
E
N
2D SD
3D AR
F
3D SD
2/2.5D SR
N
G
3D SD
2/2.5D SR
3D CR
3D AR
N
40 cm
H
3D SD-f
2/2.5D SR
N

runnels and are aligned along a NW-SE axis thus oblique according to the shoreline (Tab. 1, Fig. 3E). Their crests are almost straight and continuous. These bedforms commonly occur at the transition between the ridges and the runnels. A combined-flow (dominance of the oscillatory component) is suggested for their genesis with a mean U_o of 40–100 cm.s^{-1} and an $U_c < 4$ cm.s^{-1} (*e.g.* Harms, 1979; Dumas *et al.*, 2005; Perillo *et al.*, 2014a). They correspond to the Symmetrical Large Ripples of Dumas *et al.* (2005) and are here described as 2D Symmetrical Dunes (2D SD) according to the nomenclature of Perillo *et al.* (2014a). 2D SD can be observed superimposed by 2/2.5D SD and 3D AR (Fig. 3E), these latter being mainly preserved within the trough of the 2D SD even if some are locally present on their crest.

4.7 3D SD

Large symmetrical bedforms of *ca.* 20–50 cm high and with a wavelength of *ca.* 140 cm, are present in the runnels (Tab. 1, Fig. 3F, G and H). These bedforms have a general morphology of isolated hummocks, mainly aligned on the NW-SE and SW-NE axes. Hummocks display a dominance of rhombohedral spacing to each other, according to the classification of Allen (1985). These bedforms are most commonly located on the seaward side of the ridges slope, and preferentially at their extremities. A combined-flow (dominance of the oscillatory component) is proposed for their genesis with a mean U_o of 50–90 cm.s^{-1} and an $U_c < 20$ cm.s^{-1} (*e.g.* Harms, 1979; Dumas *et al.*, 2005; Perillo *et al.*, 2014a) even if a supercritical flow affinity could not be excluded since they share a similar aspect to the dome-like bedform described by Vaucher *et al.* (2018). They are described as 3D Symmetrical Dunes (3D SD; *sensu* Perillo *et al.*, 2014a). 3D SD are observed associated to 2/2.5D SD (Fig. 3F, G and H), to 3D AR (Fig. 3G) or 3D CR (Fig. 3G), which all are mainly preserved within the trough of the 3D SD even some are locally present on the top of the hummocks. The 3D SD often exhibits a flattened hummock part (Fig. 3H; 3D SD-f) when located close to zones with dominant USPB bedforms.

5 Discussion

5.1 Bedform genesis

The bedforms and their distributions observed at low tide slack give an overview of the processes acting during a tidal cycle. From the trough of the runnels to the crest of the ridges the following bedforms occur: 3D CR, 3D AR, 2D SR, 2D SSD, then USPB. The pattern of bedform distribution is likely the same for each couplet of ridge and runnel (Figs. 2 and 4). 3D AR and 3D CR are more frequent in the outer part of the intertidal zone. According to Dumas *et al.* (2005), Brocchini and Baldock (2008) and Perillo *et al.* (2014a) the succession of bedforms from the top of the ridge to the center of the runnel suggests a transition from oscillatory-related (USPB; 2D SSD) to oscillatory (2D SR), to combined-oscillatory dominating (3D AR), and then to unidirectional flows (3D CR). USPB results of a high flow velocity (see Tab. 1), here considered as formed by the swash and backwash of the waves on the ridges due to the collapse of the waves when their wave orbital is unsteady during decreasing water depth. 2D SSD is supposed to be formed under supercritical flow conditions either due to wave bores interaction or to backwash that both can reach supercritical conditions (Broome and Komar, 1979; Brocchini and Baldock, 2008). 2D SR needs an oscillatory flow for its formation (Tab. 1) and it can be assumed that it is formed during the same tidal state than USPB and 2D SSD. 2D SSD would be formed shallower than the 2D SR (for those having crest orientated N-S, see further in the text for an explanation). Furthermore, their position from the crest of the ridge to the slope of the runnel is always the same: USPB, 2D SSD then 2D SR (Figs. 2 and 4). 3D AR bedforms require an oscillatory dominating combined-flow for their formation (Tab. 1; Dumas *et al.*, 2005; Perillo *et al.*, 2014a). Since 3D AR are only observed without overprinted bedforms during the slack of low tide, it may be hypothesized that these bedforms are formed during the falling tide. The oscillatory motion responsible of 3D AR is wave activity, and according to their distribution (at the ridge-runnel transition), the unidirectional motion component of the combined-flow is provided by the ebb flow (see Fig. 2). 3D AR and 3D CR bedforms are mostly observed in the outer part of the intertidal zone where the ebb unidirectional flow is more important. The only pure unidirectional flow bedform generated corresponds to the 3D CR, interpreted as the final runoff of the ebb flow, which reworks material of the freshly formed 3D AR.

2D SD and 3D SD bedforms, which either are overprinted or truncated by other bedforms, are interpreted as being formed during rising tide or during the slack of high tide. The exact process responsible of their formation remains unknown even if a combined-oscillatory dominating (Tab. 1; Dumas *et al.*, 2005; Perillo *et al.*, 2014a) or supercritical flows can be suggested (Vaucher *et al.*, 2018). 2D SD and 3D SD bedforms are commonly named hydraulic dunes with current process affinities (*e.g.* Chauhan, 2000; Gallagher, 2003; Swales *et al.*, 2006; Larsen *et al.*, 2015). However, these bedforms tend to be formed in the intertidal zone of Berck-Plage only when the incoming wave reach a significant height, and are therefore linked to wave action rather than to current processes (*e.g.* Dabrio, 1982; Chauhan, 2000). Similar observations are provided by Vaucher *et al.* (2018). During the slack of high

Fig. 3. Bedforms and associated bedforms in the field. (A) 3D Current Ripples; (B) 3D Asymmetrical Ripples; (C) 2/2.5 D Symmetrical ripples; (D) 2D Small Symmetrical Dunes in the center of the residual channel are associated with 3D Current Ripples (on left) and Upper Stage Plane Bed (on the right); (E) 2D symmetrical Dunes associated with 3D Asymmetrical Ripples and Upper Stage Plane is also present on top right corner (white bar in the red circle in 20 cm); (F) 3D Symmetrical Dunes associated to 2/2.5 D Symmetrical ripples in the troughs (person for scale is 1.75 m high); (G) Association of bedforms in a runnel at the junction of two ridges, 3D Symmetrical Dunes are covered by 2/2.5 D Symmetrical ripples, 3D Current Ripples or 3D Asymmetrical Ripples. Note that 3D CR evolve as delta-*like* sediment accumulation within the trough (doted white line); (H) 3D Symmetrical Dunes, locally the hummocks are flattened (-f) and so replaced by Upper Stage Plane Bed. 2/2.5 D Symmetrical ripples are preserved in the troughs (white bar in the red circle in 20 cm).

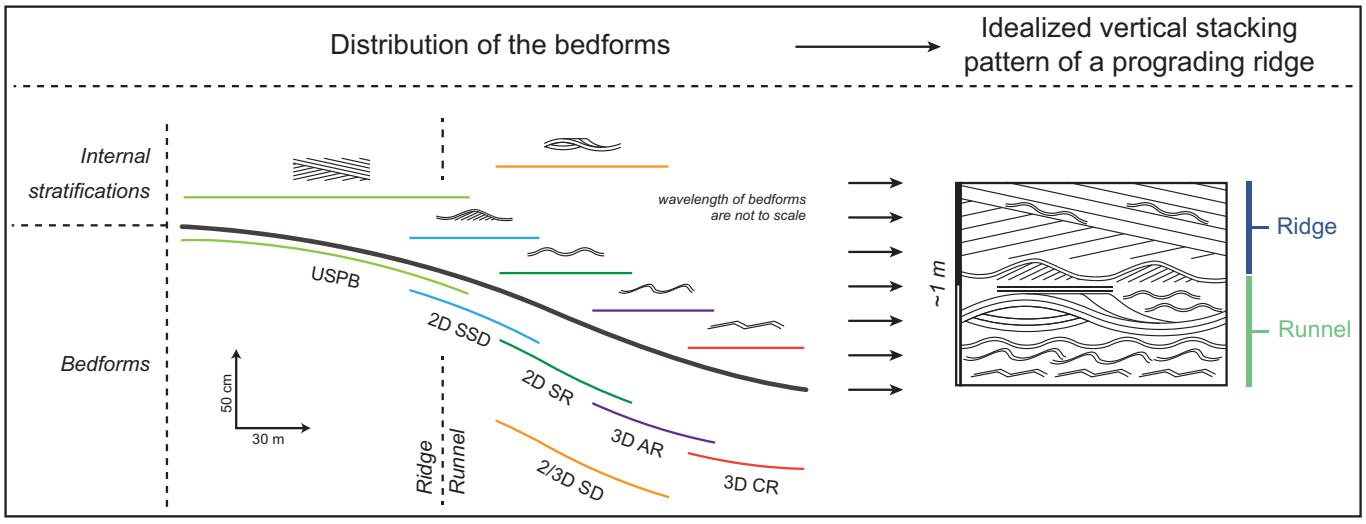

Fig. 4. Simplified representation of the intertidal ridge and runnel zone of Berck Plage, showing the distribution of the bedforms observed during the slack of low and their schematic internal stratifications. In the case of prograding ridge a vertical sacking pattern is provided giving an idealized sequence of facies.

tide, waves continuously pass over the submerged ridges and runnels, USPB is thus generated on the beach while oscillatory structures (with crests oriented N-S) are formed in the submerged intertidal zone. Larger symmetrical bedforms (*e.g.* 2D SSD) are formed when and where the water depth is reduced (crest of the ridges), while smaller oscillatory structures (*e.g.* 2D SR) are generated under more important water depth (in the trough of the runnels). Furthermore, as explained by Beji and Battjes (1993), the wave frequency increases when passing over a submerged ridge. A diminution of the wavelength of the oscillatory structures is expected to occur from the trough of the runnel to the crest of the ridges. This phenomenon implies that for the seaward ridge and runnel the wavelength of the oscillatory structures is expected to be larger than for the landward one.

The Berck-Plage intertidal zone almost exclusively (*ca.* 95%; Tab. 1) consists of wave related bedforms (except the 3D CR, which result in the runoff of the ebb flow). Dominance of oscillatory related sedimentary structures in a macro- or mega-tidal context can be explained according to Reichmüth and Anthony (2007). These latter mentioned in their study that the tidal range variation is less important than the random wave energy. By this statement Reichmüth and Anthony (2007) concluded that the longer residence time of wave processes during neap tides allows stronger offshore wave energy dissipation, while during spring tides larger waves are favoured. Consequently, in both cases, wave flow largely exceeds tide flow. This implies that the potential of preservation of sedimentary tide-related structures is weaker than those formed by waves or storms (Li *et al.*, 2000). This observation of a dominance of wave generated bedforms in a mega-tidal context have already been pointed out in a Canadian modern environment (Dashtgard *et al.*, 2009, 2012) but also recognized in the fossil record (Vaucher *et al.*, 2017).

5.2 Timing of bedform genesis

Across the intertidal zone of Berck-Plage seven bedforms were described and most of them are always found associated to other bedforms as it is shown in Figure 3. Two examples of timing of bedform genesis are highlighted in Figure 5. Close to the shoreline of highest tide, 2D SR are mainly observed within the troughs of the 3D SD and the USPB replace the hummocky part of the 3D SD (Fig. 5A). According to the vertical (temporal) pattern, the 3D SD that either are overprinted by 2D SR or by USPB, must have been generated first (during high tide). Once the falling tide starts, 2D SR are generated and thus overprint the 3D SD (Fig. 5A). The sea level is still falling, and swash and backwash process now acts on the seafloor forming USPB that flattened the zone (replacing the hummocky part of the 3D SD) and preserved the 2D SD within the trough of the 3D SD. Examples of some bedforms occurring within a runnel are given on Figure 5B. USPB is present on the top of the ridge (top left corner of the picture) while 2D SD are observed on the slope of the runnel (a grid aspect occur due to the two observed orientations of the 2D SR, N-S and E-W) and 3D AR are limited to the central part of the runnel. 3D CR are not visible on the picture but occur under the residual submerged zone (top right corner of the picture). 2D SR showing a crest orientation parallel to the runnel are considered to be formed during high tide (1 in Fig. 5) when the ridges are still submerged and that oscillatory motion is orthogonal to the shoreline. Sea level continuing to fall (2), the ridge is close to be exposed and USPB are formed on the top of the ridges. When the ridge is fully exposed the runnel still allows wave propagation and thus 2D SR are formed with crest orthogonally aligned with the runnel axis (2). The dispersion law explains this latter phenomenon (*e.g.* Landau and Lifshitz, 1987); the non-linear coastal geomorphology refracts the incoming wave, leading to wave propagation in the axis of the runnel thus generating an oscillatory motion parallel to the shore. In (3) the water is close to its lowest level; this implies that the oscillatory motion is reduced and unidirectional current increases, thus generating 3D AR and then 3D CR (when oscillatory process ceases).

In Figure 6, a stepwise cartoon is proposed to explain the spatial and temporal bedform genesis from the slack of high

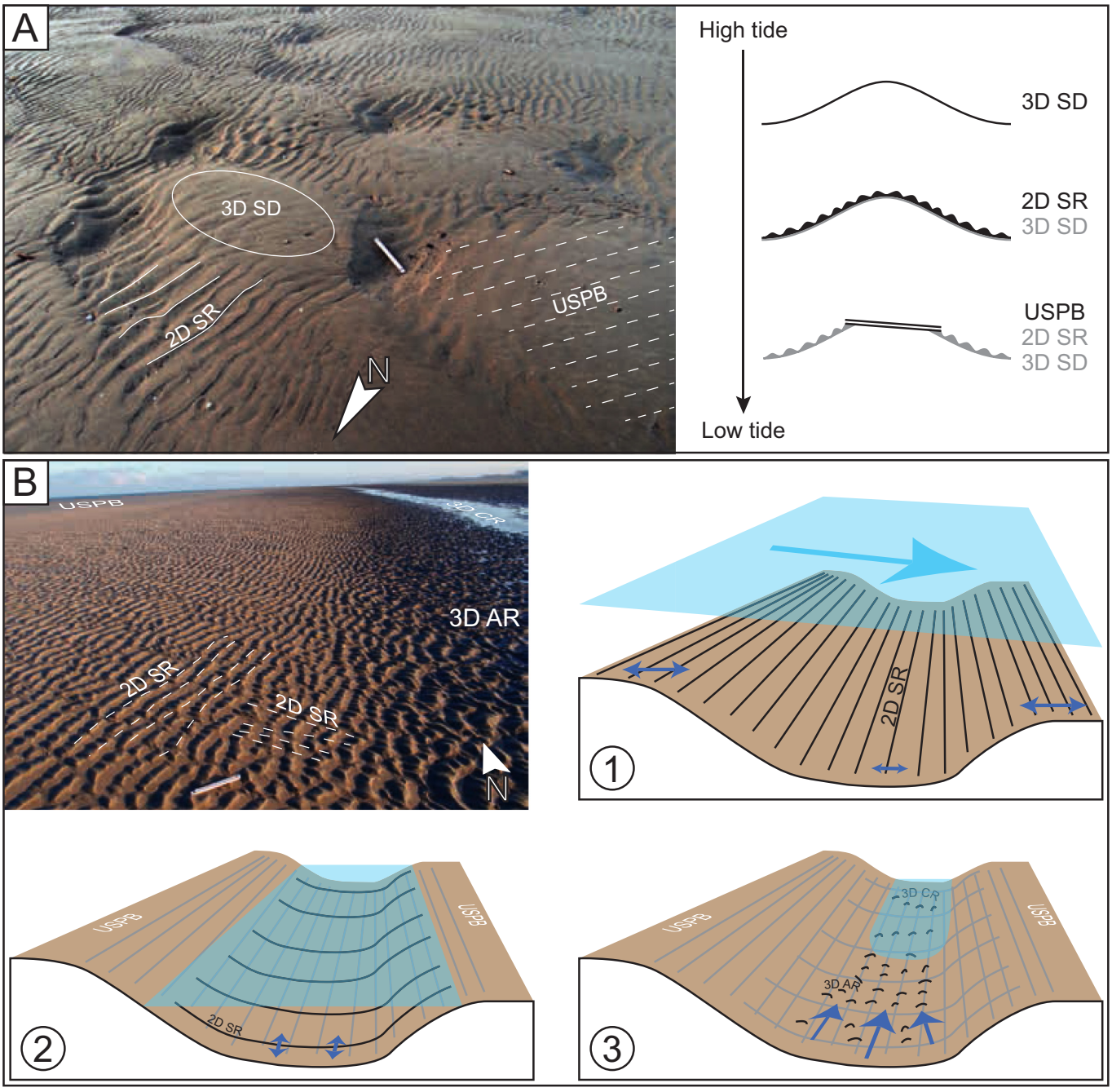

Fig. 5. (A) Bedform succession observed close to the shoreline of highest tide. 2D SR are mainly observed within the troughs of the 3D SD, and the USPB replace the hummocky part of the 3D SD. The 3D SD are generated during high tide and then, during falling tide, 2D SR are generated. Sea level continuing to fall, swash process and backwash process form USPB, flattening the zone and preserving the 2D SD within the trough of the 3D SD. (B) Bedforms occurring within a runnel. USPB is present on the ridge (top left corner) while 2D SD are observed on the slope of the runnel and 3D AR are limited to the central part of the runnel. 3D CR are not shown on the picture but occur under the small, still submerged zone. 2D SR showing an orientation parallel to the runnel are considered to be formed during high tide (1). Sea-level falling, the ridge is close to be exposed and USPB are formed on the top of the ridges (2). When the ridge is fully exposed, the runnel still allows wave propagation but now orthogonally to the shoreline. This explains how 2D SR is with crest aligned E-W (2). In (3), water is close to its lowest level and, during this step unidirectional tide current has increased, thus generating 3D AR and then 3D CR (when oscillatory process ceases).

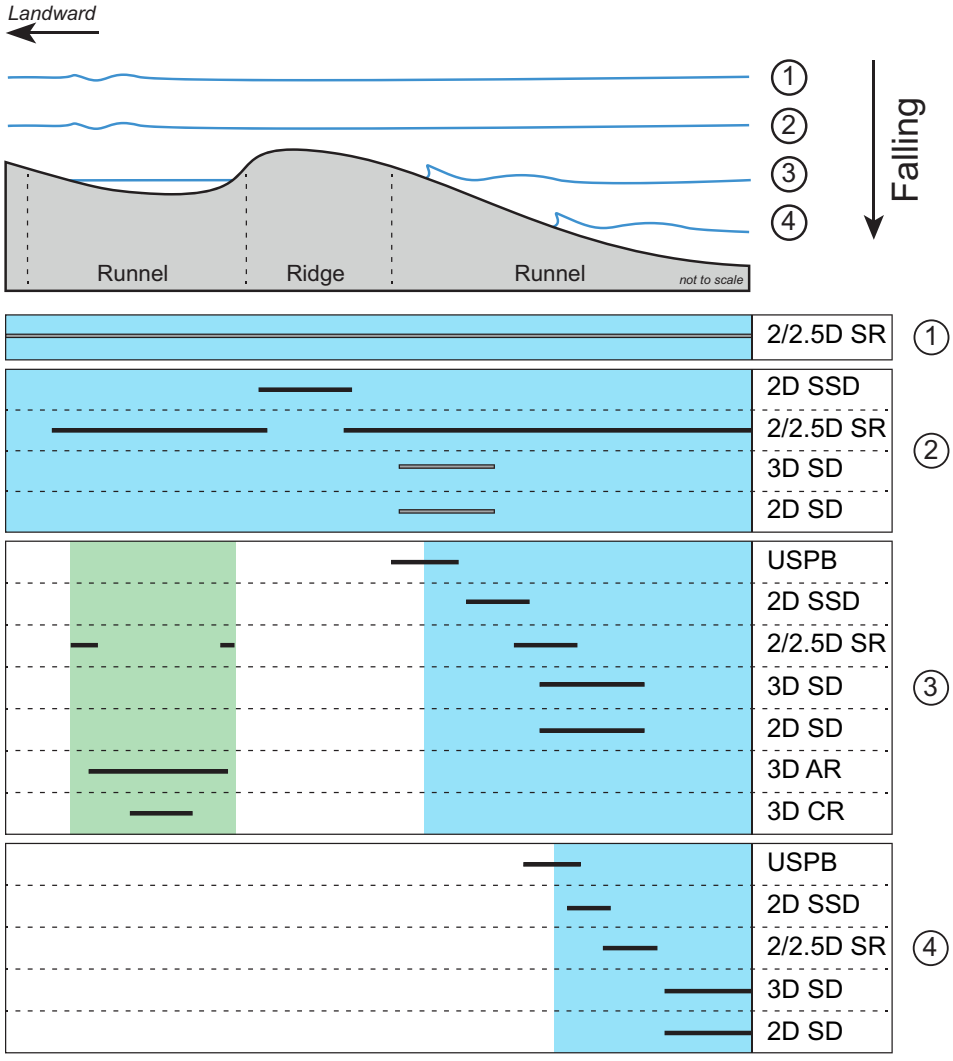

Fig. 6. Bedform generation from the slack of high tide to the slack of low tide, which focused on the last ridge, emerged during spring tide. 3D CR (3D Current Ripples); 3D AR (3D Asymmetrical Ripples); 2/2.5D SR (2/2.5D Symmetrical ripples); 2D SSD (2D Symmetrical Small Dunes); USPB (Upper Stage Plane Bed); 3D SD (3D Symmetrical Dunes); 2D SD (2D Symmetrical Dunes). Black lines correspond to demonstrated bedform occurrence. Grey lines correspond to hypothesized bedform occurrence. Blue colour corresponds to the orthogonal wave propagation according to the shoreline while the green one is for parallel propagation.

tide to the slack of low tide. During step 1 (slack of high tide; Fig. 6) the runnel-ridge-runnel zone is fully submerged, thus the incident waves mostly generate small symmetrical- quasi-asymmetrical ripples (2/2.5 SR) across the entire submerged zone (Fig. 5B). In this first step, the oscillatory motion is orthogonal to the shoreline thus the crests of the 2/2.5 SR are oriented N-S. Step 2 corresponds to the beginning of the falling tide (Fig. 6). In this second step, the ridge is still submerged but the water level has decreased and the oscillatory motion is still orthogonal to the coastline. Thus, larger symmetrical structures (2D SSD) are formed at the top of the ridges (shallower conditions) (Fig. 2), and the rest of the submerged zone is still dominated by 2/2.5D SR (deeper conditions) (Fig. 5B). The position through the intertidal zone of the 2D SD and the 3D SD (Figs. 2 and 4), which are both always superimposed by other bedforms (*e.g.* USPB, 2D SR; Figs. 3E, F, G, H and 4A) are hypothesized to be formed during the falling and/or the rising tide. In step 3, the runnels are still submerged and the ridge is now exposed. In this configuration, swash and backwash processes occur on the seaward slope of the runnel thus forming plane- or low-angle-parallel stratifications (USPB), while structures such as 2D SSD are formed by supercritical flows and oscillatory flow formed 2/2.5D SR in the deeper part of the runnel (Fig. 6). In step 3, the landward runnel plays a role of channel for the ebb-flow and a weak but still present oscillation occurs (now parallel to the coastline) thus promoting the formation of oscillatory- (2D SR with crest orientated E-W) and combined-flow ripples (3D AR) on the border of the channel and current ripples (3D CR) at its center (Fig. 6). The final step of the diagram consists of the slack of

low tide (Fig. 6). Step 4 exposed the landward runnel as well as the ridge. Swash and backwash processes still act on the seaward slope at the coastline but at a lower position than in step 3 thus moving down the zone where USPB are formed. 2D SSD and 2/2.5D SR are still formed but their area of distribution is lower and seaward than in step 3.

5.3 Theoretical sequence of facies

The bedform genesis through the falling tide shows that several successive bedforms can occur in a defined location (Figs. 5 and 6). This implies that bedforms successively generated can be theoretically be preserved as a vertical stacking pattern reflecting a sequence of facies that would characterized a prograding ridge (Fig. 4). However, their potential of preservation is extremely weak as tide and wave intensities continuously vary. The most frequently recorded bedforms would probably be the USPB as the process responsible for its formation is the most powerful of those acting on the intertidal zone, and because the position of this swash/backwash zone continuously changes along the intertidal zone during a tide cycle. These described bedforms in this study are superficial and thus potentially unrelated to the sedimentary structures preserved below the surface (*e.g.* Yang *et al.*, 2005, 2008a, b). The seven observed bedforms are generated during fair-weather condition, which implies that they could be removed during each storm and then not being recorded (Immenhauser, 2009) and thus, storm deposits could have a highest preservation potential (*e.g.* Swift and Thorne, 1991; Zhang *et al.*, 1997). The sequence of facies of the normally prograding ridge and runnel intertidal zone of Berck-Plage exhibits the different bedforms recorded in this study (Fig. 4) and a potential ancient analogues could be the Lower Ordovician sedimentary succession of Morocco (Fig. 7) (Vaucher *et al.*, 2017). Since this sequence of facies (Fig. 4) is hypothetical, all couplets of ridge and runnel as well as all encountered bedforms in Berck-Plage are not susceptible to be preserved. However, several possibilities exist in order to preserve these bedforms and the general architecture of the intertidal zone composed by ridge and runnel: (1) the cross-shore migration of the ridges (*e.g.* Ruessink and Kroon, 1994; Ruessink and Terwindt, 2000; Grunnet and Ruessink, 2005) through the intertidal zone implies that the seven bedforms can potentially be stacked together; and/or (2) a fast relative sea level rise combined with a high aggradation rate (*e.g.* Wheatcroft, 1990, Yang *et al.*, 2008a).

The recognition of such bedform pattern in an ancient sedimentary succession would be helpful for the paleoenvironmental reconstruction since they are diagnostic of wave dominated tidally influenced ridge and runnel environments but lacking of typical tidal structures (*e.g.* tidal dunes, flaser, wavy or lenticular beddings) because almost all bedforms are related of oscillation processes. Similar bedform patterns have been recognized in the Lower Ordovician sedimentary succession of Morocco (Zini Formation) (Fig. 7). The Zini Formation was deposited in a wave-dominated tide-modulated environment and exhibits very similar sedimentary structures than those described in the present study (Vaucher *et al.*, 2017). Symmetrical and slightly asymmetrical oscillatory sedimentary structures (red intervals Fig. 7A) of various sizes are sandwiched between dominantly low-angle or plane-parallel stratifications (yellow intervals Fig. 7A) (Vaucher *et al.*, 2017). As shown in Figure 2 the area of distribution of the different bedforms trough the intertidal zone of Berck-Plage is very limited. This observation could likely explain why the stratigraphic intervals dominated by symmetrical and slightly asymmetrical oscillatory sedimentary structures (corresponding to the 2D SR, 2D SD and 3D SD) exhibit a very limited lateral extension (white arrow Fig. 7A) and laterally evolve as low-angle or plane-parallel stratifications (USPB) (red-to-yellow arrow in Fig. 7A). Such vertical stacking pattern of sedimentary structures is thus interpreted as being diagnostic for a wave dominated ridge and runnel intertidal zone (Fig. 7B) (Vaucher *et al.*, 2017).

Careful observations have to be made in order to distinguish a stacking pattern of parasequence *versus* a prograding ridge and runnel system. Both in Berck Plage and in the Moroccan sedimentary succession, USPB, 2D SR, 3D AR, 2D SD and 3D SD are present, only the 3D CR and the 2D SSD are absent in Morocco. However, according to Figure 2 and Table 1, 3D CR and 2D SSD are the less frequently found bedforms in the intertidal zone of Berck Plage. For the Zini Formation, the denomination of 2D SD and 3D SD is grouped in 2/3D SD since the outcrops did not permit to make the distinction. In the case of a stack of parasequence, it would be expected to find continuous beds exclusively composed by one type of facies. This would lead to a hypothetical repeated vertical stacking pattern of five facies (USPB, 2D SR, 3D AR and 2/3D SD). However, as shown by Vaucher *et al.* (2017), the bed configuration differs (Fig. 7). In the Zini Formation (Fig. 7), beds are discontinuous at a meter-scale, and sedimentary structures evolved laterally from planar beddings to oscillatory related sedimentary structures (Fig. 7A). This lateral variability of facies is comparable to what occurs through the intertidal zone of Berck Plage (Fig. 4 and 7A). Furthermore, the Zini Formation is about 10 m thick, which is the common thickness of a megatidal intertidal zone (*e.g.* Levoy *et al.*, 2000). Based on this statement the Zini Formation defined as wave dominated tidally modulated intertidal zone could represent an ancient analogue of this study thus attesting of the potentiality of preservation of sedimentary systems like Berck Plage. Useful observations would be found in ancient sedimentary successions, oblique cross-stratifications displaying opposite sense of progradation at the base of the interval dominated by oscillatory structures. Such observations would correspond to the progradation of the 3D CR and the 3D AR having directions of progradation corresponding to the two main orientations of the ebb-flow (Fig. 2).

Until now very few hybrid sedimentary systems were described in ancient sedimentary successions (*e.g.* Basilici *et al.*, 2011, 2012; Vakarelov *et al.*, 2012; Rossi and Steel, 2016; Smosna and Bruner 2016; Vaucher *et al.*, 2017). This study however, allows to partially complete the different theoretical sedimentary successions of tidally modulated shorefaces illustrated in Dashtgard *et al.*, (2012) and described in Yang *et al.*, (2008a). The inventory of the different described bedforms of Berck-Plage provides new key criteria of recognition for ancient hybrid (wave and tide) sedimentary systems and then is helpful for paleoenvironment reconstructions.

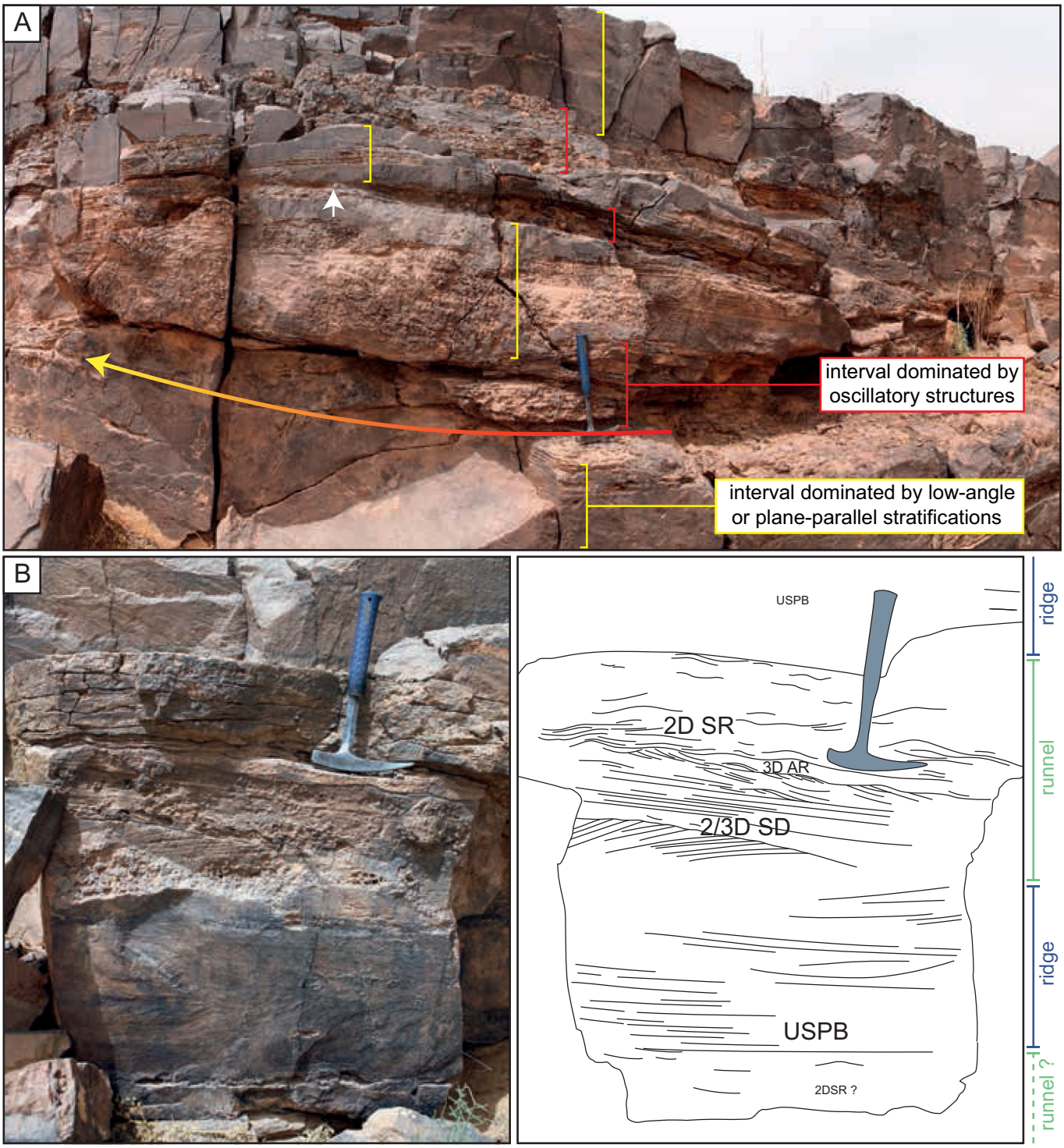

Fig. 7. The Zini Formation (Floian, Early Ordovician) outcrops in the central Anti-Atlas of Morocco (Zagora area) and is interpreted as a wave dominated ridge and runnel intertidal zone (Vaucher *et al.*, 2017). (A) The sandstones of the Zini Formation consist of an alternation of beds dominated by symmetrical and slightly asymmetrical oscillatory sedimentary structures of various sizes (red part) sandwiched between more massive beds, which mainly exhibit low-angle- or plane-parallel stratifications (yellow part). White arrow points to the limited lateral extension of oscillatory structures dominated interval. Red-to-yellow arrow shows the lateral transition from oscillatory structures dominated interval to low-angle or plane-parallel stratifications dominated interval. (B) Detailed section of the Zini Formation showing the transition between sedimentary structures characterizing the ridge part (Upper Stage Plane Beds) and the runnel part (2D Symmetrical Ripples, 3D Asymmetrical Ripples and 2D/3D Symmetrical Dunes). Scale: hammer is 32 cm long.

6 Conclusion

The study of the intertidal zone of Berck-Plage during spring tide under fair weather condition has permitted to define and to map seven types of dominant bedforms (3D current ripples; 3D asymmetrical ripples; 2D symmetrical ripples; 2D symmetrical small dunes; 2D symmetrical dunes; 3D symmetrical dunes; upper stage plane beds) observed at low tide. The analysis of the seven defined bedforms allows us to point out the flow affinities responsible of both their formation and distribution. The findings confirm the dominance of bedforms having oscillatory flow affinities even if the area was submitted to mega-tides. The survey in this area has permitted to propose a timing of formation for each encountered bedform. The stacking pattern of the bedforms is translated as a theoretical sequence of facies characterized by symmetrical and slightly asymmetrical oscillatory related sedimentary structures of various wavelengths sandwiched between dominantly low-angle or plane-parallel stratifications. Thus this sequence of facies can be applied for ancient sedimentary succession as keys of recognition for wave-dominated tidally modulated proximal environment when no pure tide generated structures are present.

Acknowledgements. We are thankful to Jean-Yves Reynaud for his sensible remarks that helped us to improve the quality of the manuscript.

References

Allen JRL. 1985. Principles of physical sedimentology. London: Allen & Unwin, 272 p.

Allen PA. 1997. Earth surface processes. London: Blackwell Science, 404 p.

Anthony EJ, Levoy F, Monfort O. 2004. Morphodynamics of intertidal bars on a megatidal beach, Merlimont, Northern France. *Marine Geology* 208(1): 73–100.

Augris C, Clabaut P, Costa S, Gourmelon F, Latteux B. 2004. Évolution morpho-sédimentaire du domaine littoral et marin de la Seine-Maritime. Conseil Général de la Seine-Maritime, EDF, 2d. Ifremer, Bilans et Perspectives, Ifremer, 159 p.

Basilici G, De Luca PHV, Oliveira EP. 2011. A depositional model for a wave-dominated open-coast tidal flat, based on analyses of the Cambrian-Ordovician Lagarto and Palmares formations, north-eastern Brazil. *Sedimentology* 59(5): 1613–1639.

Basilici G, de Luca PHV, Poire DG. 2012. Hummocky cross-stratification-like structures and combined-flow ripples in the Punta Negra Formation (Lower-Middle Devonian, Argentine Precordillera): a turbiditic deep-water or storm-dominated prodelta inner-shelf system? *Sedimentary Geology* 267: 73–92.

Beji S, Battjes JA. 1993. Experimental investigation of wave propagation over a bar. *Coastal Engineering* 19(1): 151–162.

Brocchini M, Baldock TE. 2008. Recent advances in modeling swash zone dynamics: influence of surf-swash interaction on nearshore hydrodynamics and morphodynamics. *Reviews of Geophysics* 46: RG3003. DOI: 10.1029/2006RG000215.

Broome R, Komar PD. 1979. Undular hydraulic jumps and the formation of backlash ripples on beaches. *Sedimentology* 26: 543–559.

Chauhan PPS. 2000. Bedform association on a ridge and runnel foreshore: implications for the hydrography of a macrotidal estuarine beach. *Journal of Coastal Research* 16(4): 1011–1021.

Clifton HE, Hunter RE, Phillips RL. 1971. Depositional structures and processes in the non-barred high-energy nearshore. *Journal of Sedimentary Research* 41(3): 1163–1165.

Cummings DI, Dumas S, Dalrymple RW. 2009. Fine-grained *versus* coarse-grained wave ripples generated experimentally under large-scale oscillatory flow. *Journal of Sedimentary Research* 79(1-2): 83–93.

Dabrio CJ. 1982. Sedimentary structures generated on the foreshore by migrating ridge and runnel systems on microtidal and mesotidal coasts of S. Spain. *Sedimentary Geology* 32(1-2): 141–151.

Dalrymple RW. 1992. Tidal depositional systems. In Walker RG, James NP, eds. *Facies models: response to sea level change*. St John's (Newfoundland): Geological Association of Canada, pp. 195–218.

Dalrymple RW. 2010. Tidal depositional systems. In: James NP, Dalrymple RW, eds. *Facies models 4*. St John's (Newfoundland): Geological Association of Canada, pp. 201–231.

Dalrymple RW, Baker EK, Harris PT, Hughes MG. 2003. Sedimentology and stratigraphy of a tide-dominated, foreland-basin delta (Fly River, Papua New Guinea). In Sidi FH, Nummedal D, Imbert B, Darman H, Posamentier HW, eds. *Tropical Deltas of Southeast Asia—Sedimentology, Stratigraphy, and Petroleum Geology*. Tulsa (Oklahoma): SEPM, 76, pp. 147–173.

Dashtgard SE, Gingras MK, MacEachern JA. 2009. Tidally modulated shorefaces. *Journal of Sedimentary Research* 79(11-12): 793–807.

Dashtgard SE, MacEachern JA, Frey SE, Gingras MK. 2012. Tidal effects on the shoreface: towards a conceptual framework. *Sedimentary Geology* 279: 42–61.

Davis Jr RA. 1985. Beach and nearshore zone, Coastal sedimentary environments. New York (NY): Springer New York, 379–444.

Davis Jr RA, Hayes MO. 1984. What is a wave-dominated coast? *Marine Geology* 60(1-4): 313–329.

Davis RAJ, Dalrymple RW. 2012. Principles of tidal sedimentology. Dordrecht: Springer-Verlag.

Dumas S, Arnott RWC, Southard JB. 2005. Experiments on oscillatory-flow and combined-flow bed forms: implications for interpreting parts of the shallow-marine sedimentary record. *Journal of Sedimentary Research* 75(3): 501–513.

Gallagher EL. 2003. A note on megaripples in the surf zone: evidence for their relation to steady flow dunes. *Marine Geology* 193(3-4): 171–176.

Grunnet NM, Ruessink BG. 2005. Morphodynamic response of nearshore bars to a shoreface nourishment. *Coastal Engineering* 52 (2): 119–137.

Hale PB, McCann SB. 1982. Rhythmic topography in a mesotidal, low-wave-energy environment. *Journal of Sedimentary Petrology* 52: 415–429.

Harms J. 1979. Primary sedimentary structures. *Annual Review of Earth and Planetary Sciences* 7: 227.

Immenhauser A. 2009. Estimating palaeo-water depth from the physical rock record. *Earth-Science Reviews* 96(1): 107–139.

King CAM. 1972. Beaches and Coasts, 2nd ed. London: Edward Arnold.

King CAM, Williams WW. 1949. The formation and movement of sand bars by wave action. *The Geographical Journal* 113: 70–85.

Kroon A, Masselink G. 2002. Morphodynamics of intertidal bar morphology on a macrotidal beach under low-energy wave conditions, North Lincolnshire, England. *Marine Geology* 190(3-4): 591–608.

Landau L, Lifshitz E. 1987. Fluid mechanics. 2nd ed. Oxford: Pergamon Press.

Larsen SM, Greenwood B, Aagaard T. 2015. Observations of megaripples in the surf zone. *Marine Geology* 364, 1–11.

Lashteh Neshaei MA, Holmes P, Gholipour Salimi M. 2009. A semi-empirical model for beach profile evolution in the vicinity of reflective structures. *Ocean Engineering* 36(17-18): 1303–1315.

Levoy F, Anthony E, Barusseau J-P, Howa H, Tessier B. 1998. Morphodynamique d'une plage macrotidale à barres. *Comptes*

Rendus de l'Académie des Sciences – Series IIA – Earth and Planetary Science 327(12): 811–818.
Levoy F, Anthony EJ, Monfort O, Larsonneur C. 2000. The morphodynamics of megatidal beaches in Normandy, France. *Marine Geology* 171(1-4): 39–59.
Li C, Wang P, Daidu F, Bing D, Tiesong L. 2000. Open-coast intertidal deposits and the preservation potential of individual laminae: a case study from east-central China. *Sedimentology* 47(5): 1039–1051.
Masselink G. 2004. Formation and evolution of multiple intertidal bars on macrotidal beaches: application of a morphodynamic model. *Coastal Engineering* 51(8-9): 713–730.
Masselink G, Anthony EJ. 2001. Location and height of intertidal bars on macrotidal ridge and runnel beaches. *Earth Surface Processes and Landforms* 26(7): 759–774.
Masselink G, Kroon A, Davidson-Arnott RGD. 2006. Morphodynamics of intertidal bars in wave-dominated coastal settings. A review. *Geomorphology* 73(1-2): 33–49.
McLane M. 1995. Sedimentology. Oxford: Oxford university press, 423 p.
Perillo MM, Best J, Garcia MH. 2014a. A new phase diagram for combined-flow bedforms. *Journal of Sedimentary Research* 84(4): 301–313.
Perillo MM, Best JL, Yokokawa M, Sekiguchi T, Takagawa T, Garcia MH. 2014b. A unified model for bedform development and equilibrium under unidirectional, oscillatory and combined-flows. *Sedimentology* 61(7): 2063–2085.
Perillo MM, Prokocki EW, Best JL, García MH. 2014c. Bed form genesis from bed defects under unidirectional, oscillatory, and combined flows. *Journal of Geophysical Research: Earth Surface* 119(12): 2635–2652.
Pierrot Deseilligny M. 2015. Apero, Pastis and other beverages in a nutshell! http://logiciels.ign.fr/IMG/pdf/docmicmac-2.pdf.
Pierrot Deseilligny M, Clery I. 2011. Apero, an open source bundle adjusment software for automatic calibration and orientation of set of images. *International Archives of the Photogrammetry, Remote Sensing and Spatial Information Sciences* 38: 269–276.
Plint AG. 2010. Wave-and storm-dominated shoreline and shallow-marine systems. In: Dalrymple RW, James NP, eds. *Facies models*. St John's: Geol. Assoc. Canada, pp. 167–200.
Reichmüth B, Anthony EJ. 2007. Tidal influence on the intertidal bar morphology of two contrasting macrotidal beaches. *Geomorphology* 90(1-2): 101–114.
Rossi VM, Steel RJ. 2016. The role of tidal, wave and river currents in the evolution of mixed-energy deltas: example from the Lajas Formation (Argentina). *Sedimentology* 63(4): 824–864.
Ruessink BG. 1998. The temporal and spatial variability of infragravity energy in a barred nearshore zone. *Continental Shelf Research* 18(6): 585–605.
Ruessink BG, Kroon A. 1994. The behaviour of a multiple bar system in the nearshore zone of Terschelling, the Netherlands: 1965–1993. *Marine Geology* 121(3): 187–197.
Ruessink BG, Terwindt JHJ. 2000. The behaviour of nearshore bars on the time scale of years: a conceptual model. *Marine Geology* 163(1-4): 289–302.
Short A. 1991. Macro-meso tidal beach morphodynamics: an overview. *Journal of Coastal Research* 7(2): 417–436.
Sipka V, Anthony EJ. 1999. Morphology and hydrodynamics of a macrotidal ridge and runnel beach under modal low wave conditions. *Journal de Recherche Océanographique* 24: 25–31.
Smosna R, Bruner KR. 2016. A tide-dominated beach from the cambro-ordovician cabos formation of Northwestern Spain. *Journal of Sedimentary Research* 86(12): 1378–1398.
Stépanian A, Levoy F. 2003. Séquences d'évolution morphodynamique des barres intertidales d'une plage macrotidale : l'exemple d'Omaha beach (Normandie, France). *Oceanologica Acta* 26(2): 167–177.
Swales A, Oldman JW, Smith K. 2006. Bedform geometry on a barred sandy shore. *Marine Geology* 226(3-4): 243–259.
Swift DJP, Thorne JA. 1991. Sedimentation on continental margins, I: a general model for shelf sedimentation. In: Swift DJP, Oertel GF, Tillman RW, Thorne JA, eds. *Shelf sand and sandstone bodies: geometry, facies and sequence stratigraphy. International Association of Sedimentologists, Special Publication*. 14, Oxford (UK): Blackwell Publishing Ltd. pp. 3–31.
Vakarelov BK, Ainsworth RB, MacEachern JA. 2012. Recognition of wave-dominated, tide-influenced shoreline systems in the rock record: Variations from a microtidal shoreline model. *Sedimentary Geology* 279: 23–41.
van Houwelingen S, Masselink G, Bullard J. 2006. Characteristics and dynamics of multiple intertidal bars, north Lincolnshire, England. *Earth Surface Processes and Landforms* 31(4): 428–443.
Vaucher R, Pittet B, Hormière H, Martin E, Lefebvre B. 2017. A wave-dominated, tide-modulated model for the lower ordovician of the anti-atlas, Morocco. *Sedimentology* 64(3): 777–807.
Vaucher R, Pittet B, Humbert T, Ferry S. 2018. Large-scale bedforms induced by supercritical flows and wave–wave interference in the intertidal zone (Cap Ferret, France). *Geo-Marine Letters*.
Voulgaris G, Simmonds D, Michel D, Howa H, Collins MB, Huntley DA. 1998. Measuring and modelling sediment transport on a macrotidal ridge and runnel beach: an intercomparison. *Journal of Coastal Research* 14(1): 315–330.
Wheatcroft RA. 1990. Preservation potential of sedimentary event layers. *Geology* 18(9): 843–845.
Wijnberg KM, Kroon A. 2002. Barred beaches. *Geomorphology* 48 (1-3): 103–120.
Yang BC, Chun SS. 2001. A seasonal model of surface sedimentation on the Baeksu open-coast intertidal flat, southwestern coast of Korea. *Geosciences Journal* 5(3): 251–262.
Yang BC, Dalrymple RW, Chun SS. 2005. Sedimentation on a wave-dominated, open-coast tidal flat, south-western Korea: summer tidal flat – winter shoreface. *Sedimentology* 52(2): 235–252.
Yang BC, Dalrymple RW, Chun SS. 2006. The significance of hummocky cross-stratification (HCS) wavelengths: evidence from an open-coast tidal flat, South Korea. *Journal of Sedimentary Research* 76 (1-2): 2–8.
Yang BC, Dalrymple RW, Chun SS, Johnson MF, Lee HJ. 2008a. Tidally modulated storm sedimentation on open-coast tidal flats, southwestern coast of Korea: distinguishing tidal-flat from shoreface storm deposits. In: Hampson GJ, Steel RJ, Burgess PB, Dalrymple RW, eds. *Recent advances in models of siliciclastic shallow-marine stratigraphy.* Tulsa (Oklahoma): SEPM Special Publication, 90, 161–176.
Yang BC, Gingras MK, Pemberton SG, Dalrymple RW. 2008b. Wave-generated tidal bundles as an indicator of wave-dominated tidal flats. *Geology* 36(1): 39–42.
Zhang Y, Swift DJP, Niedoroda AW, Reed CW, Thorne JA. 1997. Simulation of sedimentary facies on the northern California shelf. *Geology* 25: 635–638.

Cite this article as: Vaucher R, Pittet B, Passot S, Grandjean P, Humbert T, Allemand P. 2018. Bedforms in a tidally modulated ridge and runnel shoreface (Berck-Plage; North France): implications for the geological record, *BSGF - Earth Sciences Bulletin* 189: 5.